J. W. Hutchinson

T. J. Lu

Division of Applied Sciences,
Harvard University,
Cambridge, MA 02138

Laminate Delamination Due to Thermal Gradients

Flaw-induced delamination of orthotropic laminates subject to through-thickness temperature gradients is analyzed. A crack-like flaw impedes heat flow through the laminate, producing thermal stresses and crack tip stress intensities. The focus is on delamination cracks which propagate under steady-state conditions. The steady-state analysis becomes accurate for a crack whose length is about one laminate thickness. Moreover, the analysis provides realistic fail-safe criteria for excluding delamination.

1 Introduction

Ceramic matrix composites are being investigated for use as plate and shell components in turbine engines which involve relatively low mechanical stress but high through-thickness temperature gradients. A high temperature gradient across a thin-walled laminate does not necessarily induce significant thermal stress. However, if the laminate contains an interior crack-like flaw lying parallel to its surfaces, the flaw can impede the transverse heat flow, redistribute the temperature, and thereby induce local thermal stresses. These flaw-induced thermal stresses can be large enough to cause the flaw to become critical and spread as a delamination crack. Early work on thermally loaded cracks was carried out by Goodier and Florence (1959, 1963) and Sih (1962). These authors considered an isolated plane strain crack of length 2a in an isotropic infinite body subject to a remote temperature gradient, $\partial T/\partial z$, directed perpendicular to the crack. They assumed that no heat flows across the crack. The thermal stresses induced by the crack has a mode II crack tip field with an energy release rate given by

$$G = \frac{(1+\upsilon)\pi E a^3}{16(1-\upsilon)}\left(\alpha\frac{\partial T}{\partial z}\right)^2 \tag{1}$$

where E is Young's modulus, υ is Poisson's ratio and α is the coefficient of thermal expansion.

Subsequent work by several authors (Barber, 1979; Sturla and Barber, 1988; Kuo, 1990) has addressed other issues such as anisotropy, penny-shaped cracks versus plane strain cracks, and the effect of cracks which have less than perfect thermal insulation. The effect of a crack in an orthotropic plate supporting a temperature difference across its faces was considered by Thangjitham and Choi (1993). This is also the problem addressed in this paper. The geometry and temperature conditions are shown in Fig. 1. Plane strain conditions are assumed. Here the focus is on cracks which are sufficiently long such that a steady-state delamination analysis can be performed. This has the decided advantage that closed form results of considerable generality can be obtained. As a practical matter, it will be argued that the crack approaches steady-state delamination conditions when its length is only about one laminate thickness. Moreover, since the energy release rates of shorter cracks are less than that of the steady-state crack, the results from the steady-state analysis can be used as the basis of a fail-safe criterion to exclude delamination.

2 Steady-State Analysis

Let 2a be the length of the plane strain crack which is positioned a distance H_1 below the upper surface and H_2 above the lower surface of an infinite laminated plate of thickness $H = H_1 + H_2$, as shown in Fig. 1. The upper surface is subject to a uniform temperature T_1 and the lower surface to T_2. It is anticipated that the crack will be open (conditions such that this is the case will emerge from the analysis). The heat flow across the crack surfaces at any point is assumed to satisfy

$$q_z = h_c(T_B - T_A) \tag{2}$$

where $T_A = T(x, 0^+)$, $T_B = T(x, 0^-)$ and h_c is the conductivity across the crack interface. The conductivity depends on the heat conduction mechanisms across the crack and, in general, will depend on the crack opening. Here, as an approximation, we take h_c to be constant along the entire crack. Thus, h_c should be regarded as an effective, or average, quantity. With k_z as the thermal conductivity in the solid in the z direction, the temperature gradient on each face of the crack under steady-state heat flow must satisfy $-k_z\partial T/\partial z = q_z$. The laminate is assumed to have uniform properties and be orthotropic with respect to axes (x, y, z). The stress-strain equations relevant to the problem are

$$\epsilon_{xx} = \frac{1}{E_x}\sigma_{xx} - \frac{\upsilon_{xy}}{E_y}\sigma_{yy} - \frac{\upsilon_{xz}}{E_z}\sigma_{zz} + \alpha_x\Delta T$$

$$\epsilon_{yy} = -\frac{\upsilon_{xy}}{E_y}\sigma_{xx} + \frac{1}{E_y}\sigma_{yy} - \frac{\upsilon_{yz}}{E_z}\sigma_{zz} + \alpha_y\Delta T$$

$$\epsilon_{zz} = -\frac{\upsilon_{xz}}{E_z}\sigma_{xx} - \frac{\upsilon_{yz}}{E_z}\sigma_{yy} + \frac{1}{E_z}\sigma_{zz} + \alpha_{z\Delta T}$$

$$\epsilon_{xz} = \frac{1}{2G_{xz}}\sigma_{xz} \tag{3}$$

where without loss in generality the temperature of the lower surface is taken as reference such that $\Delta T = T - T_2$. The configuration in Fig. 1 is analyzed under the constraint of plane strain, i.e. $\epsilon_{yy} = 0$. Superposition of a uniform stress σ_{yy} does not induce any change in the singular crack tip fields. Thus, the plane strain results for the stress intensity factors and the energy release rate will apply to any generalized plane strain situation. The steady-state analysis given below will involve portions of the plate in which $\sigma_{zz} = 0$; then, with $\epsilon_{yy} = 0$,

$$\epsilon_{xx} = \left(\frac{1}{E_x} - \frac{\upsilon_{xy}^2}{E_y}\right)\sigma_{xx} + (\alpha_x + \upsilon_{xy}\alpha_y)\Delta T \equiv \frac{1}{\bar{E}}\sigma_{xx} + \bar{\alpha}\Delta T \tag{4}$$

The idea behind the analysis is to consider the limit when the crack is long ($2a \gg H$) such that the temperature and stress distributions away from the ends of the crack depend only on z. Once these distributions have been identified, the energy release rate and stress intensity factors can then be obtained from a previous analysis given for the general loading in Fig. 2 by Suo (1990) and Hutchinson and Suo (1992). In regions

Contributed by the Materials Division for Publication in the JOURNAL OF ENGINEERING MATERIALS AND TECHNOLOGY. Manuscript received by the Materials Division May 5, 1995. Associate Technical Editor: G. J. Weng.

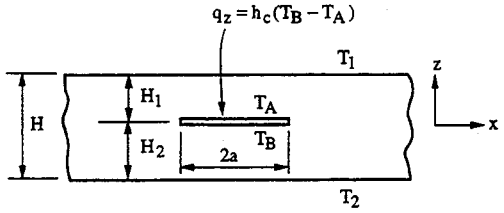

Fig. 1 Notation and conventions for a laminate containing a plane strain crack under thermal loading

of the laminate well away from the ends of the crack the steady-state temperature distributions are linear in z within each layer. In the uncracked laminate well to the right of the tip,

$$T = (T_1 - T_2)z/H + (H_1T_2 + H_2T_1)/H \tag{5}$$

In the central cracked region away from the crack tips,

$$T = (T_1 - T_A)z/H_1 + T_A \quad \text{for} \quad z > 0$$
$$T = (T_B - T_2)z/H_2 + T_B \quad \text{for} \quad z < 0 \tag{6}$$

where T_A and T_B are the temperatures at the upper and lower surfaces of the crack. These are

$$T_A = \frac{T_1(1+\eta) + B_c(T_1 + \eta T_2)}{(1+B_c)(1+\eta)} \quad \text{and}$$
$$T_B = \frac{T_2(1+\eta) + B_c(T_1 + \eta T_2)}{(1+B_c)(1+\eta)} \tag{7}$$

with $\eta = H_1/H_2$ and $B_c = Hh_c/k_z$. The temperature jump across the crack is given by

$$T_A - T_B = \frac{T_1 - T_2}{1 + B_c} \tag{8}$$

such that the heat flow impeded by the crack is $q_z/(1 + B_c)$. The dimensionless Biot number, B_c, controls the heat flow across the crack surfaces. In the limit, $B_c = 0$, the crack is perfectly insulating such that $T_A = T_1$ and $T_B = T_2$. At the other extreme when $B_c \to \infty$, there is no interruption of the heat flow by the crack, $T_A = T_B = (T_1 + \eta T_2)/(1 + \eta)$, and (6) reduces to (5).

As indicated in Fig. 2, let P be the force (per unit depth in the y-direction) carried by the layers of the laminate above and below the crack, and let M_1 and M_2 be the moments (per unit depth) carried by the layers about their respective midplanes with the positive senses shown. The stress distribution in each of the layers well away from the tip is

$$\sigma_{xx} = -\frac{P}{H_1} + \frac{M_1}{I_1}\left(z - \frac{H_1}{2}\right) \quad \text{for} \quad z > 0$$
$$\sigma_{xx} = \frac{P}{H_2} + \frac{M_2}{I_2}\left(z + \frac{H_2}{2}\right) \quad \text{for} \quad z < 0 \tag{9}$$

where $I_1 = H_1^3/12$ and $I_2 = H_2^3/12$. The distribution of the strain ϵ_{xx} is given by (4) in terms of the distribution of σ_{xx} and T in the respective layers. Equilibrium requires $M_2 = -M_1 + PH/2$. The conditions for determining the remaining two unknowns, P and M_1, are the two compatibility requirements for layer segments in central portions of the plate away from the crack tips: (i) equality of the curvatures of the upper and lower layers, κ_1 and κ_2, and (ii) equality of the strain components on the crack surfaces, i.e. $\epsilon_{xx}(z = 0^+) = \epsilon_{xx}(z = 0^-)$. These are asymptotic conditions which must be approached in the central sections in steady-state limit as a/H becomes large. Were they not met, the two layers would not join up at the crack tip. That is, as longer and longer cracks are considered, any other conditions in the central sections would be incompatible with a steady-state solution. Imposition of these two conditions gives

$$P = \frac{\bar{E}\bar{\alpha}H(T_1 - T_2)}{(1+B_c)}\frac{\eta(1+\eta^3)}{(1+\eta)^5}$$
$$M_1 = \frac{\eta^3}{2(1+\eta^3)}PH, \quad M_2 = M_1/\eta^3 \tag{10}$$

All the information needed to evaluate the energy release rate and the mode I and II stress intensity factors has now been assembled. With reference to Section III of Hutchinson and Suo (1992), the desired results are:

$$\frac{G}{\bar{E}H[\bar{\alpha}(T_1 - T_2)]^2} = \frac{\eta(1+\eta^3)}{2(1+B_c)^2(1+\eta)^5} \tag{11}$$

$$\frac{K_I}{\bar{E}\sqrt{H}\bar{\alpha}(T_1 - T_2)} = F\lambda^{1/4}\left\{\frac{\cos\omega}{\sqrt{U}} - \frac{\eta^2(1+\eta)}{2(1+\eta^3)}\frac{\sin(\omega+\gamma)}{\sqrt{V}}\right\}$$

$$\frac{K_{II}}{\bar{E}\sqrt{H}\bar{\alpha}(T_1 - T_2)} = F\left\{\frac{\sin\omega}{\sqrt{U}} + \frac{\eta^2(1+\eta)}{2(1+\eta^3)}\frac{\cos(\omega+\gamma)}{\sqrt{V}}\right\} \tag{12}$$

where

$$F = \frac{\lambda^{1/2}}{[2(1+\rho)]^{1/4}}\frac{\sqrt{\eta}(1+\eta^3)}{(1+B_c)(1+\eta)^{9/2}} \quad \lambda = \frac{E_z}{E_x}$$
$$\frac{1}{U} = 1 + 4\eta + 6\eta^2 + 3\eta^3 \quad \frac{1}{V} = 12(1+\eta^3)$$
$$\rho = \frac{(E_x/E_z)^{1/2}}{G_{xz}} - \upsilon_{xz} \quad \frac{\sin\gamma}{\sqrt{UV}} = 6\eta^2(1+\eta)$$
$$\omega \cong 52.1 - 3\eta \text{ (in degrees)} \tag{13}$$

The measure ψ of the relative amount of mode II to mode I is given by

$$\tan\psi \equiv \frac{K_{II}}{K_I} = \lambda^{-1/4}$$
$$\times \frac{2(1+\eta^3)\sqrt{V}\sin\omega + \eta^2(1+\eta)\sqrt{U}\cos(\omega+\gamma)}{2(1+\eta^3)\sqrt{V}\cos\omega - \eta^2(1+\eta)\sqrt{U}\sin(\omega+\gamma)} \tag{14}$$

In carrying out the above analysis, it has been assumed that the crack is open and that K_I is positive. The parameter regime for which this assumption is met will be seen in the next section.

3 Results and Implications

To see the relevance of the steady-state solutions, denote the steady-state energy release rate given by (11) by $G_{\text{steady-state}}$ and denote the short crack limit in (1) by $G_{\text{short crack}}$. When the crack length $2a$ is very short compared to H, the temperature gradient $\partial T/\partial z$ in (1) should be identified with $(T_1 - T_2)/H$. With this replacement, the ratio of the two estimates of the energy release

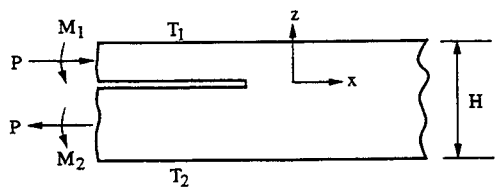

Fig. 2 Section of a laminate with a "long" crack. Axial forces and moments, per unit width in the y-direction, are applied at the two left edges.

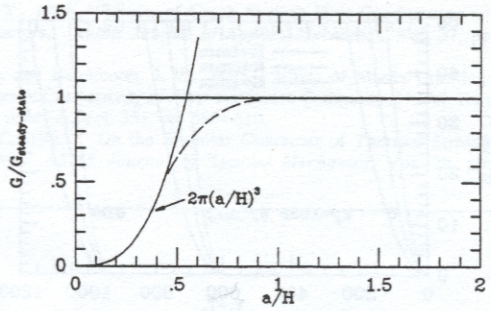

Fig. 3 Transition of energy release rate from short crack limit to steady state for a perfectly insulating crack ($B_c = 0$) located on the midplane ($\eta = 1$)

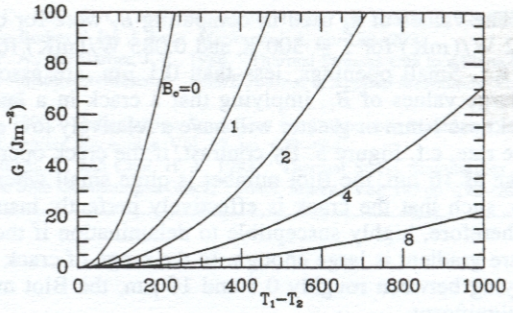

Fig. 5 Effect of Biot number, B_c, on energy release rate with increasing temperature loading, $T_1 - T_2$, for steady-state cracking in alumina ($H_1/H = 0.211$, $H = 2$ mm)

rate for a laminate with isotropic properties and a perfectly insulating crack ($B_c = 0$), positioned halfway between the upper and lower surfaces of the laminate ($\eta = 1$), is

$$\frac{G_{\text{short crack}}}{G_{\text{steady-state}}} = 2\pi\left(\frac{a}{H}\right)^3 \tag{15}$$

The expected trend showing the transition from (15) to steady-state is indicated by a dashed curve in Fig. 3. Steady-state behavior should be in force at a crack length, $2a$, which is just over one plate thickness H. Equally important, the steady-state energy release rate is expected to be the maximum release rate possible. Thus, if conditions are such that the steady-state energy release rate is below the delamination toughness, $\Gamma_c(\psi)$, extensive delamination cannot occur. In this sense, the steady-state analysis provides a fail safe criterion. Because the energy release rate in the short crack limit is so strongly dependent of the crack length, increasing in proportion to a^3, cracks much shorter than about a laminate thickness will be subject to driving forces well below the steady-state limit. This suggests that flaws of concern will be those whose size exceeds about a laminate thickness.

Curves for the steady-state energy release rate as a function of the depth of the crack below the top surface from (11) are shown in Fig. 4(a) for an isotropic laminate. Companion results

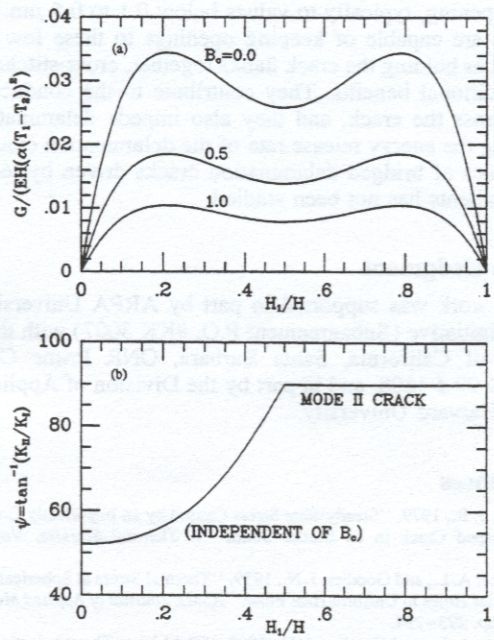

Fig. 4 (*a*) Steady-state energy release rate G, and (*b*) measure of mode mixity ψ as functions of crack position H_1/H for an isotropic plate with various B_c values. $T_1 > T_2$

for ψ for the tip at the right end of the crack are given in Fig. 4(b). The measure of the mode mixity is independent of the Biot number, B_c. For $T_1 > T_2$, for which the curve in Fig. 4b applies, the crack tip is open with a positive mode I stress intensity factor as long as the crack lies above the midplane of the laminate. The crack tip is closed and is in pure mode II when the crack lies below the midplane. The present analysis does not apply when the crack is closed. Nevertheless, the energy release rate may not be greatly in error in this regime if frictional interaction between the crack faces can be neglected. Since the delamination toughness of a closed crack under pure mode-II is generally larger than that of a crack tip experiencing some opening, the likelihood of a crack forming on the cooler side of the midsurface is small anyway. Cracks located approximately one quarter of a laminate thickness below the hot surface ($H_1/H = 0.211$, to be precise) experience the highest energy release-rate and a small, but not insignificant, positive mode I stress intensity component. It is near this location that delamination cracks are most likely to lie.

The energy release-rates associated with thermal delamination can be fairly large, as the following numerical example illustrates. Consider an isotropic plate of alumina with the following representative properties and temperature loading:

$$\text{E} = 200 \text{ GPa}, \quad \alpha = 8 \times 10^{-6}/°\text{C},$$

$$\upsilon = 0.25, H = 2 \text{ mm}, \quad T_1 - T_2 = 500°\text{C}$$

If the crack is perfectly insulating ($B_c = 0$), the steady-state energy release rate from (11) for a crack positioned halfway between the top surface and the midplane is $G = 333.3 \text{ Jm}^{-2}$. This value far exceeds the fracture toughness of most ceramic matrix materials. Large energy release rates have been found in detailed analyses of penny-shaped cracks in representative laminate shell components of ceramic matrix composites (H. Rajiyah, G. E. Research Labs., private communication). The assumption of a perfectly insulating crack may often be too extreme, as can be seen in Fig. 5 where the energy release rate from (11) for steady-state cracking in alumina is plotted as a function of $(T_1 - T_2)$ for various B_c, with H_1/H fixed at 0.211.

The important role of the heat transfer across the crack is determined by the dimensionless Biot number, B_c, as evident in (11) and Fig. 5. At temperatures below about 1500 K the dominant mechanism of heat transfer across an open crack is due to gaseous transport. Using estimates for h_c given for gaseous transport (see Lu and Hutchinson, 1995 for values and references), one can estimate B_c. The approximate formula for B_c when δ is larger than about 0.1 μm is $B_c = k_g H/k_z \delta$ where k_g is the thermal conductivity of the gas. Fig. 6 displays plots of B_c as a function of the crack opening displacement δ for a laminate thickness $H = 1$ mm at $T = 300$ K and $T = 1273$ K, respectively, and for a composite having a transverse thermal conductivity $k_z = 30 \text{ W/(m} \cdot \text{K)}$, typical of Al_2O_3-based mate-

rials. The values of k_g used in computing B_c were for dry air (0.032 W/(mK) for T = 300 K and 0.085 W/(mK) for T = 1273 K). Small openings, less than 0.1 μm, are associated with large values of B_c, implying that a crack in a laminate of thickness 1 mm or greater will have a relatively low energy release rate, c.f. Figure 5. By contrast, if the crack opening is as large as 10 μm, the Biot number is quite small when H = 1 mm, such that the crack is effectively perfectly insulating and, therefore, highly susceptible to delamination if the temperature gradient is large enough. In the range of crack openings lying between roughly 0.1 and 10 μm, the Biot number B_c is significant.

It is revealing to relate the crack opening displacement δ to the energy release rate G and then to eliminate B_c as an unknown in (11). To this end, the relation between δ and G for a crack of length $2a$ lying along one of the principal directions of an orthotropic, infinite solid will be used as an approximation, i.e.,

$$\delta = \frac{4\lambda^{-3/4} n \cos\psi}{\sqrt{\pi}} \sqrt{\frac{Ga}{\bar{E}}} \tag{16}$$

where $n = \sqrt{(1+\rho)/2}$ and the result of Sih et al. (1965) has been used. The factor $\cos\psi$ reflects the fact that only the mode I component of crack tip intensity contributes to the opening. From Fig. 4(b) it can be noted $\cos\psi$ will be between 0.5 and 0.6 for a crack lying midway between the hot side and the center of the laminate. Notice that $\lambda = \rho = 1$ if the laminate is transversely isotropic, c.f. Eq. (13). Next,

$$B_c = \frac{k_g H}{k_z \delta} = \frac{k_g H}{4k_z \lambda^{-3/4} n \cos\psi} \sqrt{\frac{\pi \bar{E}}{Ga}} \tag{17}$$

Then, eliminating B_c in (11) gives the following relation between G and $T_1 - T_2$, assuming the crack is located at H_1/H = 0.211:

$$\left(1 + \frac{k_g H}{4k_z \lambda^{-3/4} n \cos\psi} \sqrt{\frac{\pi \bar{E}}{Ga}}\right)^2 G = 4.168 \times 10^{-2} \bar{E} H [\bar{\alpha}(T_1 - T_2)]^2 \tag{18}$$

The above relation between G and the temperature loading is displayed in Fig. 7 for alumina with the properties cited earlier (and $\lambda = \rho = 1$) for three different values of the gas conductivity parameter k_g. In this plot, the crack length, $2a$, has been taken equal to the laminate thickness H. The surprising feature of these curves is the fact that once $T_1 - T_2$ exceeds the threshold, below which G is essentially zero, G immediately becomes very large for relatively small further increases in $T_1 - T_2$. Thus, the threshold $(T_1 - T_2)_c$ associated with $G \to 0$ can serve as a conservative, but not unrealistic, measure of maximum temperature difference the laminate can sustain

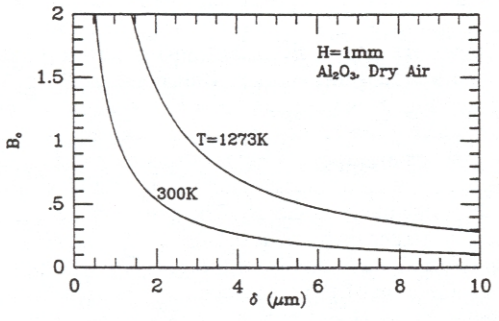

Fig. 6 Biot number, B_c, plotted as a function of crack opening displacement, δ, for dry air at two temperatures. The parameters used for plotting are H = 1 mm and k_z = 30 W/(m K)

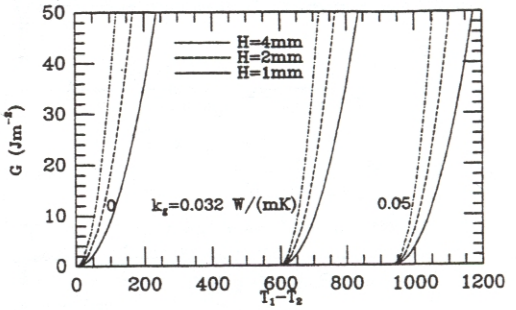

Fig. 7 Energy release rate for steady-state cracking in alumina (H_1/H = 0.211) plotted as a function of temperature loading, $T_1 - T_2$, for various values of plate thickness H and gas conductivity k_g

without delamination. This threshold from (18) is immediately seen to be

$$(T_1 - T_2)_c = 2.127 \frac{k_g}{\bar{\alpha} k_z \lambda^{-3/4} n \cos\psi} \sqrt{\frac{H}{a}} \tag{19}$$

If one further assumes that cracks of length on the order of the laminate thickness are present ($2a = H$), then this criterion simplifies even further to

$$(T_1 - T_2)_c \cong \frac{3k_g}{\bar{\alpha} k_z \lambda^{-3/4} n \cos\psi} \tag{20}$$

The threshold temperature difference increases with the temperature at the crack since the conductivity of the gas k_g increases with temperature. If the threshold exceeds the imposed temperature difference, delamination cracking is not expected to occur. As indicated by the above discussion, the heat conducted across the crack may indeed be significant, and the assumption of a perfectly insulating crack may be unduly conservative. Secondary loads, which result in bending, may enlarge the crack opening and further reduce the heat transfer across the crack. If the imposed temperature difference exceeds the threshold (20), or if secondary loads bring the crack to its critical delamination condition, steps will have to be taken to hold down the crack opening, typically to values below 0.1 to 0.5 μm. Cross-stitches are capable of keeping openings to these low levels. As well as holding the crack flanks together, cross-stitches have two additional benefits. They contribute to the conduction of heat across the crack, and they also impede delamination by reducing the energy release rate of the delamination crack. The mechanics of bridged delamination cracks driven by temperature gradients has not been studied.

Acknowledgment

This work was supported in part by ARPA University Research Initiative (Subagreement P.O. #KK 3007) with the University of California, Santa Barbara, ONR Prime Contract N00014-92-J-1808, and in part by the Division of Applied Sciences, Harvard University.

References

Barber, J. R., 1979, "Steady-state Stress Caused by an Imperfectly Conducting Penny-Shaped Crack in an Elastic Solid," *J. Thermal Stresses*, Vol. 3, pp. 77–83.

Florence, A. L., and Goodier, J. N., 1959, "Thermal Stress at Spherical Cavities and Circular Holes in Uniform Heat Flow," *ASME Journal of Applied Mechanics*, Vol. 26, pp. 293–294.

Florence, A. L., and Goodier, J. N., 1963, "The Linear Thermoelastic Problem of Uniform Heat Flow Disturbed by a Penny-Shaped Insulated Crack," *Int. J. Eng. Sci.*, Vol. 1, pp. 533–540.

Hutchinson, J. W., and Suo, Z., 1992, "Mixed Mode Cracking in Layered Materials," *Advances in Appl. Mech.*, Vol. 29, pp. 63–191.

Kuo, A.-Y., 1988, "Effects of Crack Surface Heat Conductance on Stress Intensity Factors," *ASME Journal of Applied Mechanics,* Vol. 57, pp. 354–358.

Lu, T. J., and Hutchinson, J. W., 1995, "Effect of Matrix Cracking on the Overall Thermal Conductivity of Fiber-reinforced Composites," *Phil. Trans. Roy. Soc. Lond.,* series A, Vol. 351, pp. 595–610.

Sih, G. C., 1962, "On the Singular Character of Thermal Stresses Near a Crack Tip," *ASME Journal of Applied Mechanics,* Vol. 29, pp. 587–589.

Sih, G. C., Paris, P. C., and Irwin, G. R., 1965, "On Cracks in Reclilinearly Anisotropic Bodies," *Int. J. Frac. Mech.,* Vol. 1, pp. 189–203.

Sturla, F. A., and Barber, J. R., 1988, "Thermal Stresses Due to a Plane Crack in General Anisotropic Material," *ASME Journal of Applied Mechanics,* Vol. 55, pp. 372–376.

Suo, Z., 1990, "Delamination Specimens for Orthotropic Materials," *ASME Journal of Applied Mechanics,* Vol. 57, pp. 627–634.

Thangjitham, S., and Choi, H. J., 1993, "Thermal Stress Singularities in an Anisotropic Slab Containing a Crack," *Mech. Mater.,* Vol. 14, pp. 223–238.